Sequential Gaussian Simulation of High Dimensional Stationary Data

Miguel Cuba and Oy Leuangthong

Realizations simulated using sequential Gaussian simulation SGS do not account for local features of the domain. In the case of SGS the variogram model characterizes the spatial continuity of the domain on average. If the simulated model is intended to be used for planning in relatively small periods of time e.g. for medium or short term mine plans, it should characterize the local features of the domain. This proposes a methodology for accounting for local features in a domain via SGS. It is shown how to use a high dimensional conditioning data which has been prepared to behave stationary for simulating a domain. The methodology consists of simulating the domain in a high dimensional space under stationary conditions and after that project the results to the original dimensional space of the domain. The results show that local anisotropic features of the domain are reproduced without compromising any condition of the multi-gaussian assumption.

Introduction

The influence in the experimental variogram of highly variable sub-regions in the domain can be identified and removed (Cuba & Leuangthong, Experimental variogram cleaning, 2009). The resulting cleaned experimental variogram is fitted to get a variogram model and this represents the spatial continuity of the rest of the domain without the influence of the highly variable sub-regions. Therefore, the variability of the highly variable sub-regions is not accounted for by the cleaned variogram model. Consequently, this variogram may tend to be more continuous in presence of highly variable sub-regions. The conditional distributions of the data locations in these sub-regions are not properly represented by the conventional variogram model, and even less so by the cleaned variogram model.

In (Cuba & Leuangthong, Conditional distribution fitting, 2009) it is proposed a methodology to fix the conditional distributions at these locations by separating them from the rest of the conditioning data, and then adding extra dimensions to the initial Euclidean space in order to inject more uncertainty to the conditional distributions. The resulting spatial configuration is a high dimensional version of the initial conditional data or alternative conditioning data (ACD), that behaves more stationary than in the initial space or of the original conditioning data (OCD) in that the conditional distributions properly account for local uncertainty.

In this document, this new, high dimensional dataset is used to simulate geostatistical realizations of the domain. Transferring the highly dimensional information to the domain and an alternative representation of anisotropy that does not rely on the conventional elliptic pattern are discussed. After getting a high dimensional state of the conditioning dataset and transferring that information to the domain, virtually any conventional approach can be applied to reproduce the non-stationary features related to the intrinsic assumption of the RF.

Proposed spatial analysis and approximation of additional dimensions

To show and compare the proposed approach, a real dataset is used. Specifically, the Jura dataset (Goovaerts, 1997) consists of 100 data points placed over a fairly regular grid configuration (see Figure 1). This particular data configuration helps to get a better experimental variogram without using large tolerances and also to highlight the differences between the conventional and the proposed dimensional modeling approaches. The element analyzed is Cobalt (Co). The data values are transformed to normal scores for sequential Gaussian simulation and it is assumed there is no presence of trends in either the mean or the variance.

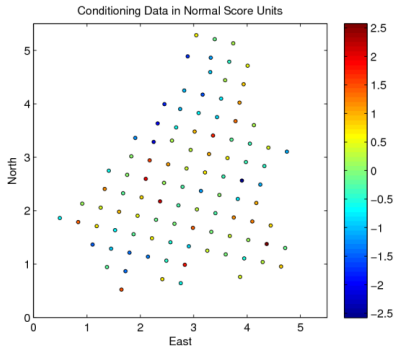

Figure 1: Configuration of the Jura dataset of Co variable in normal score units

The direction of major continuity is calculated at 45 degrees azimuth based on contour lines plotted from a variogram map (see Figure 2). The proposed variogram model consists of two anisotropic structures, both can be fit as exponential structures (see Figure 3). The first structure is isotropic with range equal to 0.6 distance units and the second one is anisotropic with the major axis equal to 5.0 units and minor axis is equal to 0.6 units (1).

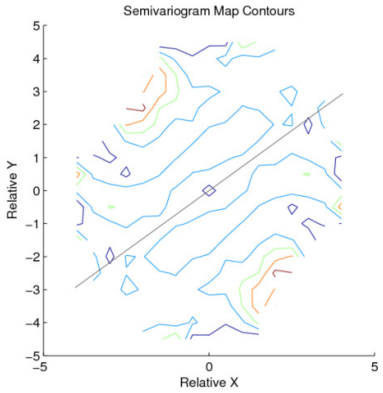

Figure 2: Variogram map of NS Co

$$\gamma(\mathbf{h}) = 0.6Exp_{\substack{mj=0.6 \\ mn=0.6}}(\mathbf{h}) + 0.4Exp_{\substack{mj=5.0 \\ mn=0.6}}(\mathbf{h}) \quad (1)$$

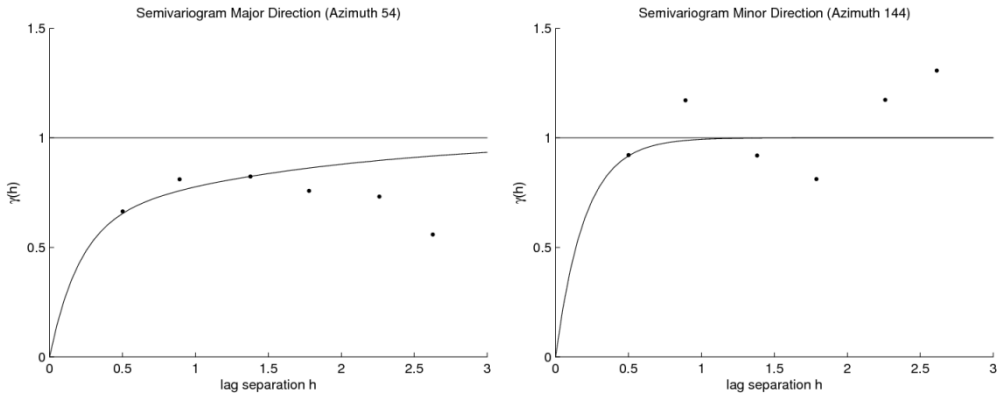

Figure 3: Variogram model (solid lines) and experimental variograms (black dots) of major (left) and minor direction (right)

The experimental variogram of the OCD is cleaned using a 99% probability cut-off. For the 2D case, both the control limit and the variogram model are surfaces. The control limit splits the cloud variogram in two parts. The first part contains the valid increments of the experimental variogram and the second part the outlier increments. The latter represents the impact of the variability of the high variable sub-regions in

the domain. The cleaned experimental variogram is calculated using the valid increments in order to eliminate the influence of the highly variable sub-regions if they exist (see Figure 4).

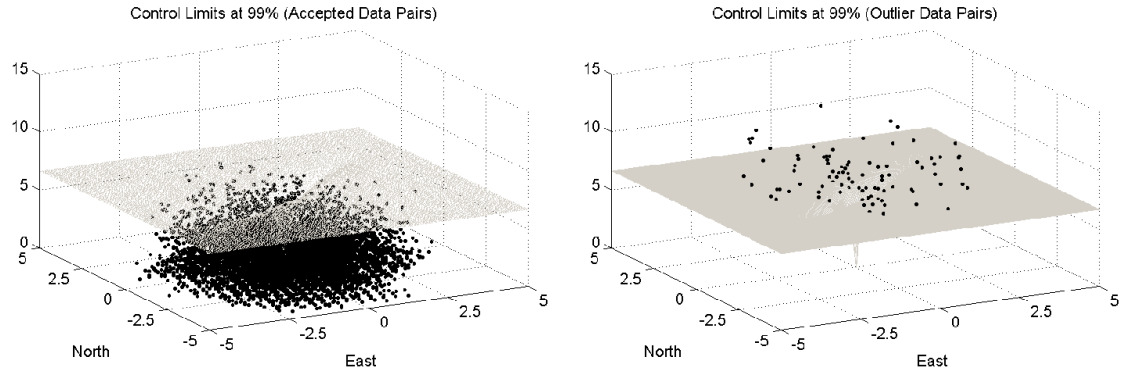

Figure 4: Cloud variogram split in two parts by a control limit at 99% probability, valid increments (left) and outlier increments (right)

In presence of highly variable regions in the domain some significant changes in the cloud variogram may result. Those changes might lead to differences in the main anisotropic orientations, the use of different variogram model for fitting the cleaned experimental variogram and larger ranges of the new variogram model. For this dataset, the differences in the experimental variogram values are too minor to support the use of a different variogram model (see Figure 5) or a different anisotropic configuration (see Figure 6).

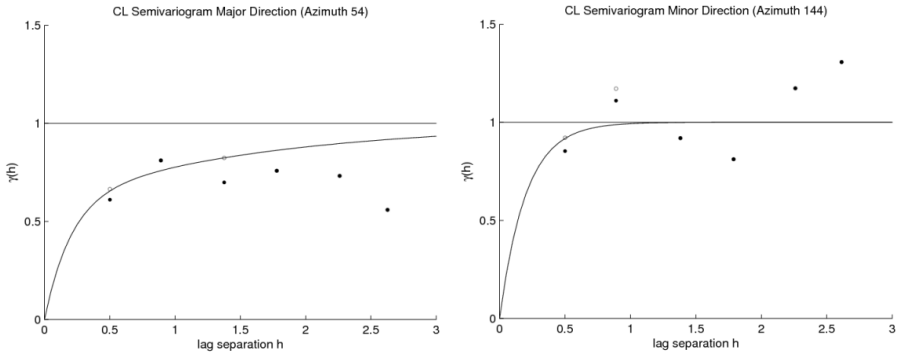

Figure 5: Variogram model (solid lines) and Experimental variograms (black dots) of major (left) and minor direction (right) after experimental variogram cleaning at 99% probability cut-off (black dots) and original experimental variogram points (empty gray dots)

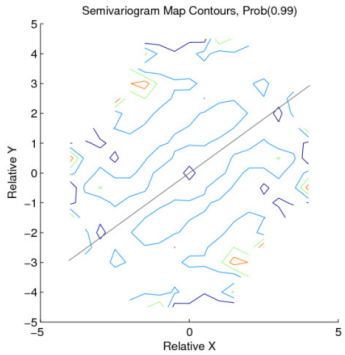

Figure 6: Variogram map after cleaning increment outliers at 99% probability

The locations of the data grouped in the outlier data pairs are plotted in Figure 7. The size of the black dots in the map represents the proportions of the number of times each sample location participates in the outlier increments, the data locations with large occurrences can be considered as problematic locations during modeling because they make large increments occur in the experimental variogram. This information can be used to identify sub-patterns in the domain that may cause problems when modeling

the variable of interest. The sample locations with small occurrences are not considered as indicators of potential sub-domains. In Figure 7 there is a group of problematic data locations on the west side that may be separated into a sub-domain, however, the frequency of those locations are relatively small compared to the two more problematic locations in the east and south-east region. For the present case study no sub-domaining is considered.

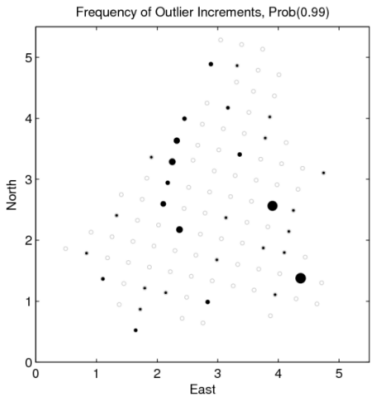

Figure 7: Occurrences of data locations that make outlier data pairs for a cut-off probability of 99%

Transferring ACD high-dimensional information into the domain

In order to be able to use the ACD in estimation/simulation, the domain of the geologic deposit has to be in the same dimensional space as the ACD. The process of moving the domain from $\mathbb{R}^n$ to $\mathbb{R}^m, \forall\, m > n$ has to be bijective. This is important for two reasons: 1) after estimating and/or simulating in $\mathbb{R}^m$ the model of the domain is analysed and studied in the OCD space, that is, $\mathbb{R}^n$; and 2) there has to be a unique correspondence between $\mathbb{R}^m$ and $\mathbb{R}^n$ because the OCD has to be exactly reproduced in the domain. The latter means the ACD projected in $\mathbb{R}^n$ has to be the OCD and no other in order to ensure the exact reproduction of the conditioning data in the domain.

The process of moving the domain from $\mathbb{R}^n$ to $\mathbb{R}^m$ consist of moving the nodes that represent the domain, each node has to have the same dimensions as the ACD. However, the values of the extra dimensions at the node locations are unknown and the process of transferring the extra dimension of the ACD can be subject to many interpretations. The extra dimensions can be seen as summarizing extra physical information about the domain and would be more convenient if they are modeled as such. This results in an additional estimation/simulation problem to get the extra dimensions at the nodes of the domain.

When modeling a mineral deposit, an outlier increment is the result of an abrupt change in the metal grade values of the data pair that is uncommon in the rest of the domain. If the problematic locations cannot be separated into another sub-domain, the outlier increments may occur because of the presence of a minor geologic structure within the domain, such as veins or faults that are difficult to separate into sub-domains because of their small scale (see Figure 8). For example, in a Cu skarn deposit, such an abrupt transition might be due to the presence of a boundary between chalcopyrite ($\mathrm{CuFeS_2}$) and bornite ($\mathrm{Cu_5FeS_4}$) minerals. When the deposit is separated in domains, both are classified as exoskarn.

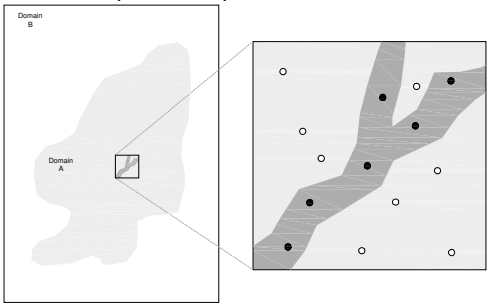

Figure 8: Sketch of a sub-structure (right) identified using outlier increments present in a large domain (left), samples with extra dimension (black dots) show the presence of an anomaly in Domain A when compared to the rest of the samples (empty dots)

Consider two data points with values in normal score units at locations $\mathbf{u1}$ and $\mathbf{u2}$ that make an outlier data pair (see Figure 9 top left). The outlier data pair implies that for this particular increment the averaged variogram model $\gamma(\mathbf{d})$ is not representative locally and the same is also assumed to be valid for the locations in between. The node locations of the domain have to be projected in the same higher dimensional space as the ACD prior to estimation/simulation. However, the only known locations in the high-dimensional space are the ones that correspond to the ACD (see Figure 9 bottom left). They are taken as reference for the transformation.

The technique proposed for transformation takes each of the extra dimensions of the ACD, one at a time, and consider them as additional variables to predict. That is, keeping the original dimensional space of the OCD make the dimensions the new variables to predict at the grid node locations. After all the dimensions are modeled in the domain as additional variables, it is assumed the domain is in the higher dimensional space. The transition of each extra dimension in the domain between sample locations in the original space can be modeled considering many different scenarios. For example, they can be modeled considering a linear transition, parabolic, convex, etc., also using geological interpretations of the extra dimension based on the fact they represent physical properties of the domain (see Figure 9 case1-4). Also, geostatistics can be used to model them. Therefore, the uncertainty associated to the extra dimensions can be introduced to the model. However, this might give unrealistic results because of the assumption of stationarity. The extra dimensions are the non-stationary part of the domain, and are only located in specific regions of the domain. Each extra dimension is not present throughout the domain because they would then become part of the random variability and can be captured by the nugget effect in the conventional experimental variogram.

Assigning predefined shapes of transitions may introduce bias due to the subjectivity of the decision. The most simplistic way to transfer the extra dimensions is the linear transition which in 2D and 3D original spaces is triangulation (see Figure 9 top middle). The advantage of triangulation is simplicity in terms of parameters. This is suitable when knowledge of the physical characteristics of the extra dimensions in the domain is lacking. Many techniques are available for implementing triangulation such as Delaunay triangulation algorithm which can be used in 2D and 3D with no problems. However, it may still be necessary to define boundaries of influence for the triangulation algorithm, which control the influence of the extra dimensions in the domain. These boundaries can be generated using nearest neighbour techniques.

The previous approach only gives one scenario of the dimensions. However, modeling the uncertainty associated to the extra dimensions would also be required. The lack of knowledge of the physical properties may lead to an unsuitable modeling approach of the dimensions. As mentioned before conventional geostatistics is inappropriate for modeling the extra dimensions because the extra dimensions cannot be assumed as part of a SRF. Any modeling technique that accounts for physical parameters would be more appropriate. Finally, the decision between the simplistic and geologically more realistic approach involves a high price when the complexity of the domain is modeled. However, a mineral deposit is of such complexity and it becomes more important when locally consistent models are required.

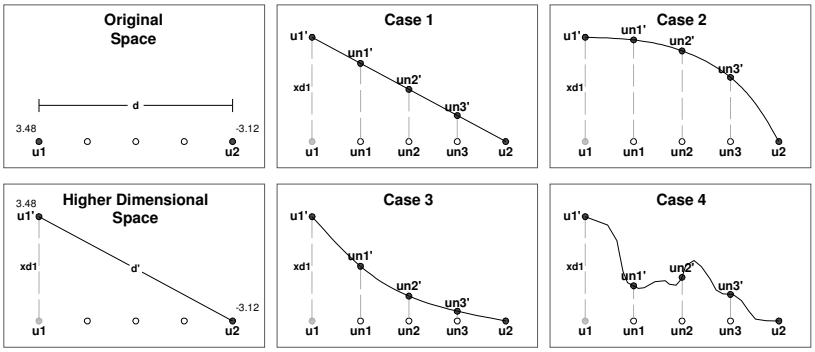

Figure 9: Sketches of cases of transferring extra dimension into grid nodes locations (empty dots), five transition cases are presented: linear (top middle), convex (top right), linear (bottom left), concave (bottom middle) and irregular (bottom right)

For the case study the extra dimensions are calculated considering a 95% probability confidence interval of the conditional distributions. One solution of the ACD dataset is found using five extra dimensions, and a triangulation technique using influence boundaries is considered for modeling the dimensions in the domain. The boundary is used to limit the influence of the extra dimensions (see Figure 10).

The new location vectors of the domain grid nodes are the combination of the initial location vectors and extra dimensions modeled in the five maps. Recall that the location vector of the ACD is the combination of the initial location vector and the extra dimensions. However, only one of the extra dimensions has a value greater than zero. In (Cuba & Leuangthong, Conditional distribution fitting, 2009) this condition was set up for simplicity. Since the new location vectors are the combination of the initial location vectors and the additional models of extra dimensions, the new location vectors of the nodes may end up having more than one extra dimensional component with values greater than zero. This is still valid and there is no problem associated to the consistency of the dimensional space.

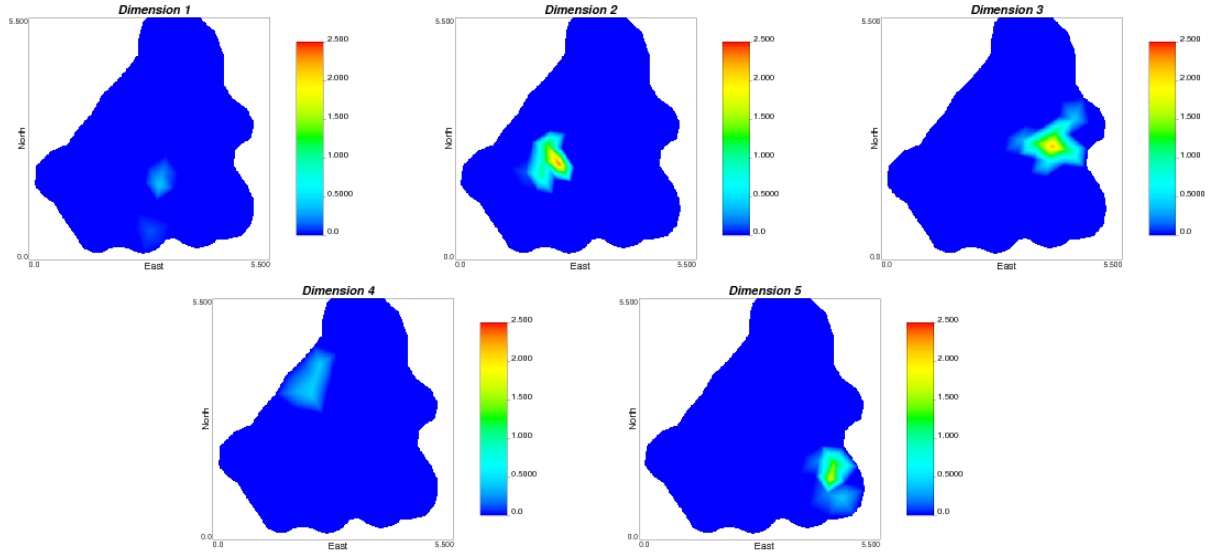

Figure 10: ACD extra dimensions transferred to domain node locations using a triangulation algorithm

After estimating/simulating in the high dimensional space the results have to be returned to the initial space to analyze the results. To do this, the estimated/simulated nodes of the domain are projected into the initial space by simply making all the extra dimensions equal to zero. There are no two node locations in the higher dimensional space that, after the projection in the initial space, fall in the same position because the components of the initial dimension remain the same. No matter the combination of the extra dimensions, the initial components will remain the same and that guarantees the bijective feature of the dimensional transformation of the domain. Consider a surface in a Euclidean $\mathbb{R}^3$ space, where X and Y axes correspond to east and north respectively and Z to elevation. If the surface is sampled over a regular grid for projecting in a XY $\mathbb{R}^2$ plane, Z simply becomes zero and there is no problem in the projection because there are no two similar combinations of X and Y in $\mathbb{R}^3$. If the projection is made over the plane XZ or YZ the projection will result in non-unique projections because there are similar values of X and Y for the projected planes respectively. In the case of the domains in hyper-dimensional space the same logic is applied, as long as there is a unique vector of the initial space, the rest of the components will not make the projection problematic.

Anisotropy in Original and Alternative Dimensional Spaces

The Euclidean space is considered as an isotropic environment because the measure of the distances is not preferential in any direction. On the other hand, an anisotropic environment can be seen as a deformation of a Euclidean space in some particular directions. The distance between two points in this case becomes a function of these anisotropic directions. A simple form of anisotropy is the ellipsoidal pattern. In $\mathbb{R}^3$ the preferential directions are defined by the three axes of the ellipsoid. They are usually referred to as major, minor and vertical axes. This form of regular shape anisotropy is suitable to be used

in conventional geostatistics because of the assumption second order stationarity of the IRF $\gamma(\mathbf{h}) = \gamma(-\mathbf{h})$. Assuming an ellipsoidal anisotropic environment the separation vector $\mathbf{h}$ can be scaled by a square matrix $\mathbf{A}$ (Isaaks & Srivastava, 1989):

$$\mathbf{h}_a = \mathbf{A} \times \mathbf{h} \tag{2}$$

The form of the anisotropic scaling matrix for any number of dimensions is (3):

$$\mathbf{A} = \left[a_{i,j} \middle| \begin{matrix} a_{i,j} = t_i, i = j \\ a_{i,j} = 0 \text{ elsewhere} \end{matrix} \right], \forall i, j \in \{1, \ldots, n\} \tag{3}$$

The diagonal elements of the anisotropy matrix are the scaling factors for each dimension of the separation vector $\mathbf{h}$. The t_i factors in the anisotropy matrix $\mathbf{A}$ scale the elements of the separation vector $\mathbf{h}$ linearly, each anisotropic component of the separation vector $\mathbf{h}_a$ is $h_{ai} = t_i h_i$. In the case of conventional estimation/simulation the problem is finding the scaling factors of the elements of the location vectors $\mathbf{u}$ that make the spatial continuity of the new scaled space be defined by the proposed variogram in its isotropic form for each of the nested structures. The anisotropic deformation of the distances is inversely proportional to the variogram anisotropic scheme. In the direction of major continuity the anisotropic distance has to be reduced in order to increase the covariance value and conversely in the direction of minor continuity. That is, $t_i = 1/q_i$, where q_i is the length of the anisotropic variogram ellipsoid axis that corresponds to dimension i.

An anisotropic scheme defined in $\mathbb{R}^n$ does not affect the extra elements of a separation vector $\mathbf{h}$ in $\mathbb{R}^m, \forall\, m > n$. The anisotropic matrix can be expanded to a higher dimension m by simply equalling the size of matrix $\mathbf{A}$ to the new total number of dimensions and adding one in the diagonal extra elements. That makes the new extra components remain the same $h_{ai} = 1h_i$.

The anisotropic matrix $\mathbf{A}$ deforms the original space in the directions of the elements of the $\mathbf{h}$ vector. However, the anisotropic ellipsoid can also involve rotation in space. The vector $\mathbf{h}$ can be rotated by multiplying it by a rotation matrix $\mathbf{R}$ (4). The form of the rotation matrix for any number of dimensions is (5); it rotates the plane of dimensions a, b (Aguilera & Pérez-Aguila, 2004). Notice the rotation directions are based on the order of the dimensions a, b. That is, θ is positive or counter-clockwise for plane a, b and negative or clockwise for plane b, a. The rotation matrix $\mathbf{R}$ can be the resulting combination of different rotated planes. This is done by rotating vector $\mathbf{h}$ by each of the different planar rotation matrices.

$$\mathbf{h}_r = \mathbf{R} \times \mathbf{h} \tag{4}$$

$$\mathbf{R}_{a,b} = \left[r_{i,j} \middle| \begin{matrix} r_{a,a} = \cos\theta \\ r_{b,b} = \cos\theta \\ r_{a,b} = -\sin\theta \\ r_{b,a} = \sin\theta \\ r_{j,j} = 1,\ j \neq a,\ j \neq b \\ r_{i,j} = 0 \text{ elsewhere} \end{matrix} \right] \tag{5}$$

The rotation matrix $\mathbf{A}$ rotates vector $\mathbf{h}$ according to the specific rotation angles. However, the system is meant to be rotated rather than the vector. For rotating the system the vector $\mathbf{h}$ is multiplied by the transpose of the rotation matrix (6). Finally, the spatial configuration of the anisotropic ellipsoid is integrated by multiplying the transpose of the rotation matrix $\mathbf{R}$ and the anisotropic matrix $\mathbf{A}$ (7). Recall that $\mathbf{RA}$ affects the vector, whereas $(\mathbf{RA})^T$ affects the system. This is consistent with the anisotropic effect in the separation vector $\mathbf{h}$ in GsLib (Deutsch & Journel, 1998). There is no limit in the number of dimensions for accounting for anisotropy and it is easy to write programming code in the matrix form.

$$\mathbf{h}_s = \mathbf{S} \times \mathbf{h} = \mathbf{R}^T \times \mathbf{h} \tag{6}$$

$$\mathbf{h}_{as} = \left(\mathbf{RA}\right)^T \mathbf{h} \tag{7}$$

The following is a 2D example of accounting for anisotropy for a separation vector $\mathbf{h}$:

$$\mathbf{h}_{as} = \left(\begin{bmatrix} \cos\theta & -\sin\theta \\ \sin\theta & \cos\theta \end{bmatrix} \begin{bmatrix} t_x & 0 \\ 0 & t_y \end{bmatrix} \right)^T \begin{bmatrix} h_x \\ h_y \end{bmatrix}$$

$$= \left(\begin{bmatrix} t_x \cos\theta & -t_y \sin\theta \\ t_x \sin\theta & t_y \cos\theta \end{bmatrix} \right)^T \begin{bmatrix} h_x \\ h_y \end{bmatrix}$$

$$= \begin{bmatrix} t_x \cos\theta & t_x \sin\theta \\ -t_y \sin\theta & t_y \cos\theta \end{bmatrix} \begin{bmatrix} h_x \\ h_y \end{bmatrix}$$

Notice that after rotating and deforming the system the new elements of the separation vector are a function of the scaling factors that correspond to each dimension $h_{ax} = t_x\left(h_x\cos\theta + h_y\sin\theta\right)$ and $h_{ay} = t_y\left(-h_x\sin\theta + h_y\cos\theta\right)$.

In practice, because of the different geologic events that formed the mineral deposit, the ideal scenario of linear estimator is one which accounts for locally different and of irregular-shape anisotropic patterns. Performing conventional estimation/simulation in such a complex environment would be virtually intractable. Even when a mineralized region has been exposed to a folding event it does not necessarily mean the anisotropic distances must be measured along the fold in order to get a better estimate. In such a situation, some approaches may consider unfolding the dimensional space of the domain. However, this may suggests that the unfolded domain is fairly stationary for estimation/simulation. A stationary environment in a high dimensional space when projected in the initial dimensional space can account for these irregular anisotropic patterns. The extra dimensions provide the necessary customized deformations in the initial dimensional space and at the same time the estimated conditional distributions account properly for both global and local uncertainty. Let us consider nine data point locations placed over a regular grid (see Figure 11). An isotropic pattern is compared to three anisotropy cases that are the result of adding one extra dimension to some of the nine sample point locations (see Figure 11). The values of the maps represent the distances measured from the center of the map to the rest of the locations. For the first case the distances are measured in the 2D plane directly. The second case corresponds to the sampling of data #6 which requires an extra dimension of length 5 units (see Figure 12-top right). For the third case, the previous configuration is kept and to sample data #1, we must assign an extra dimension of 2.5 units (see Figure 12-bottom left). Finally, for the fourth case, the configuration of case 2 is kept and sampling data #7 requires an extra dimension of 1.75 (see Figure 12-bottom right). For the three anisotropic cases only one extra dimension is used to modify the initial 2D space and a triangulation scheme is used to transfer the influence of the extra dimensions in the domain. Notice, projecting from a 3D surface to a 2D plane is sufficient for getting irregular anisotropic patterns in 2D. Recall that the extra dimensions account for the variability that cannot be represented in the initial space.

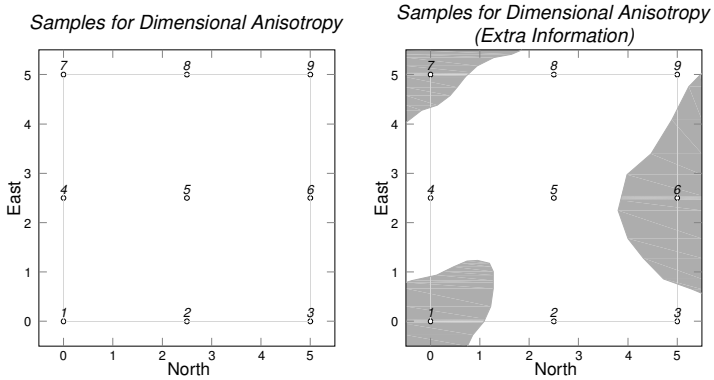

Figure 11: Initial configuration of nine data point locations in 2D for showing the effect of irregular shaped anisotropic patterns

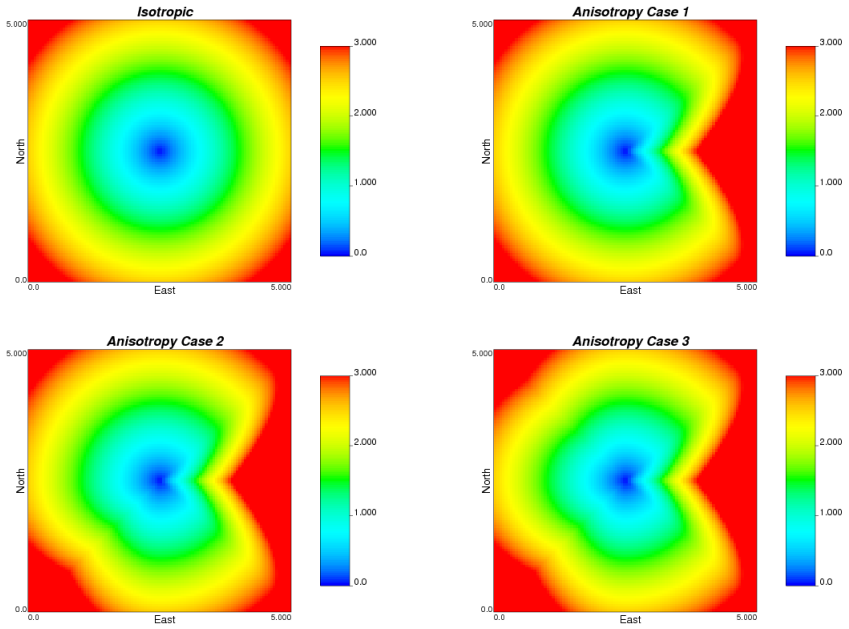

Figure 12: Comparison of an isotropic pattern (top left) against three cases of irregular shape anisotropic patterns with one sample with an extra dimension (top right), two samples with extra dimension (bottom left) and three samples with extra dimension (bottom right)

The irregular anisotropic patterns account for the locations in the domain where the local uncertainty is under-estimated. The irregular anisotropic patterns are more flexible than conventional regular ones. Even when they can vary locally there is still the problem related to the symmetry of the anisotropic pattern. Samples that are located in one side of the location to estimate have to have exactly the same influence as the samples on the opposite side. In the conventional approach the influence of the surrounding conditioning data cannot be customized even in presence of geologic information that supports such decision. The additional information that might support irregularities in the symmetric influence of conditioning data can be extra geologic information. Recall that considering the variable to model is a regionalized variable and that any additional information is disregarded from the modeling process unless a co-regionalization environment is considered. However, co-regionalization considers dependence between primary and secondary variables, the dependence of the variable of interest might not be direct with each of the secondary variables one-by-one but a relationship of the primary variable with a combination of the rest of the variables. In Figure 11-left, for estimating/simulating at location #5 the conventional approach considers the spatial continuity is only a function of the variable of interest, whereas the domain usually has additional features that control the continuity variable of interest.

Comparison between Conventional and Proposed Approach.

The conventional approach shares the same anisotropic pattern all along the domain as a result of assuming second order stationarity. As a result, the model may be unrealistic because the estimates capture a global uncertainty, whereas the local features remain averaged. However, both the conventional and the proposed approach rely on the assumption of multi-gaussianity and reproduces features, such as variogram and global distribution (see Figure 13). For comparing the experimental variogram reproduction between the conventional and the dimensional approach, in the case of the latter only part of the domain share the same dimensional locations, that is, the regions where the extra dimensions are zero. Recall that the location vectors of the nodes affected by the extra dimensions (see Figure 10) are not the same as in the original space XY. Therefore, the experimental variograms calculated in the plane XY do not consider such node locations. From the total of 75625 nodes in the original dimensional space without considering any boundaries 58331 are not affected by the dimensional approach. The experimental variograms of the realizations in the dimensional approach (see Figure 13 top-left) are supported by the 58331 node locations, whereas, the experimental variograms of the

conventional approach by 75625 nodes, this is one of the reasons why the experimental variograms reproduction of the dimensional approach looks more variable. In the case of the verification of the global distribution reproduction (see Figure 13 bottom) all the 75625 nodes are considered because this verification is not dimensional dependent.

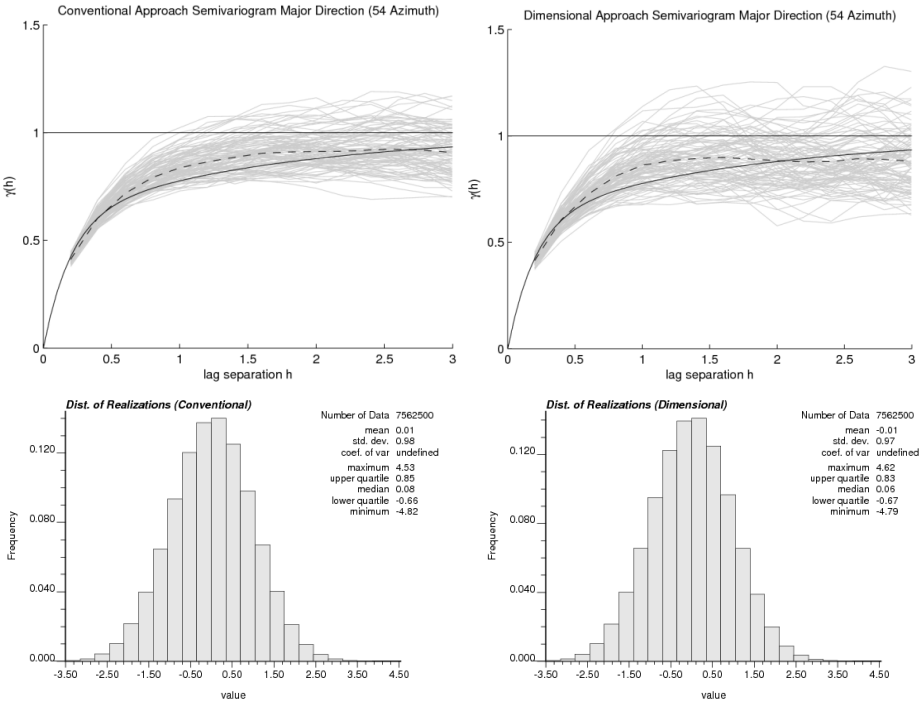

Figure 13: Experimental variogram and global distribution reproduction of 100 realizations for conventional approach (left side) and dimensional approach (right side)

The simulated nodes in the dimensional approach because of the deformation of the initial space reproduce non-stationary features of the variogram when projected in the initial dimension (see Figure 14-right). The conventional approach shows a constant anisotropic pattern along the domain (see Figure 14-left). In both cases the standard normal distribution is reproduced. In the conventional approach the variogram is reproduced in the initial space, however, as mentioned initially the variogram is not fully representative of the domain in the initial space and there is no reason for this. The approach relies on the domain being stationary in a hyper space; in that space the variogram is reproduced and the anisotropic patterns are constant.

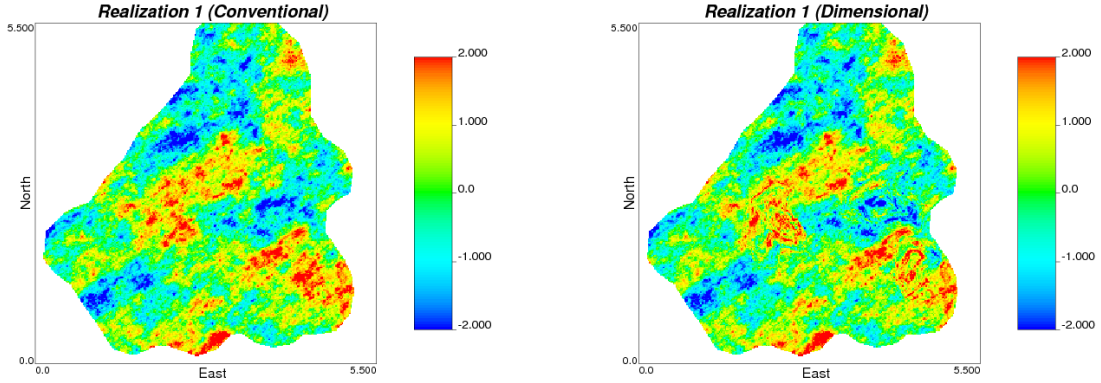

Figure 14: First realization using conventional simulation (left) and dimensional proposed approach (right)

After averaging many realizations the conditional estimated means for the dimensional approach also reproduce the non-stationary features as the realization maps and in the conventional approach the anisotropic pattern is constant (see Figure 15). Notice in the dimensional approach the data locations that were identified in the variogram analysis stage as problematic locations are not spread in the domain. The

problematic data locations are extreme values either positive or negative. They become problematic when the samples that surround them are so different that the increments cannot be accounted by the variogram model, therefore the conditional distribution is under-estimated.

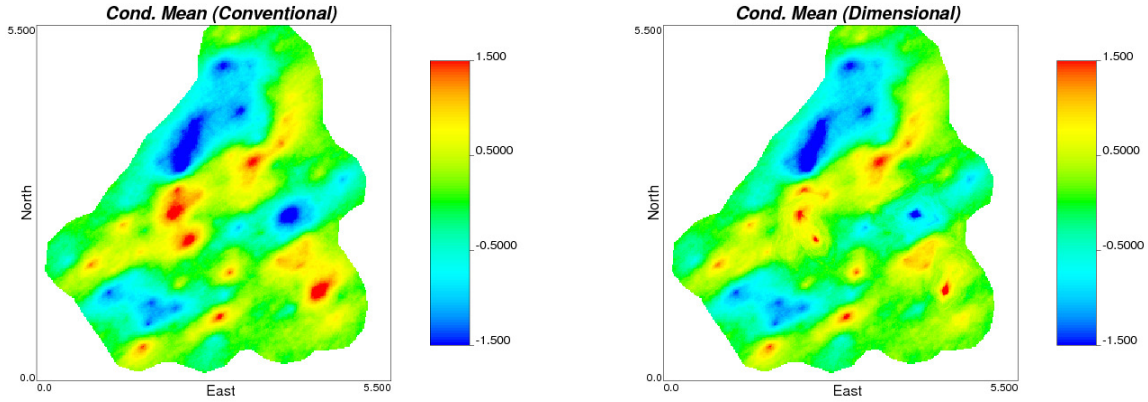

Figure 15: E-type map of 100 realizations in normal score units of conventional approach (left) and dimensional proposed approach (right)

The difference of the conditional means between the conventional and the dimensional approach for this exercise shows there is a preferential trend to constrain the higher values rather than lower values (see Figure 16). There is no condition that makes the mean of the distributions is centered to zero or the distribution is unbiased. It is a function of the occurrence of the problematic locations. The map of the differences shows that most of the regions constrain the high values and only in one region the influence of a low value sample is limited (see Figure 15 left).

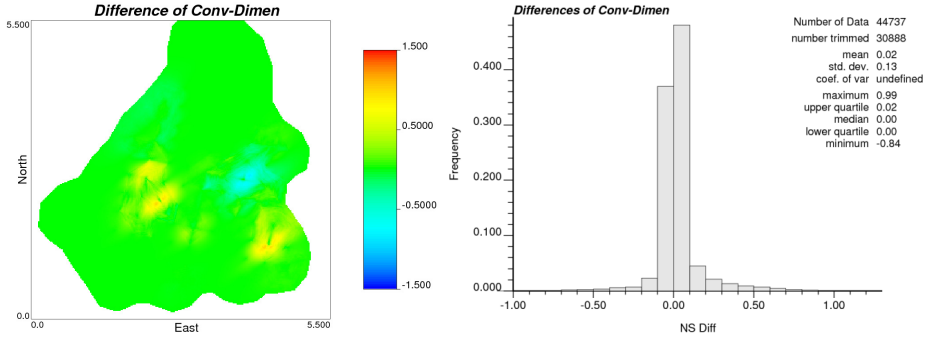

Figure 16: Map (left) and distribution (right) of difference between conventional and dimensional means.

The conditional variances are data configuration dependent; they are almost similar for regular configuration patterns of the conditioning data. In the example presented the conditioning data is placed fairly over a regular grid, the conditional variances are also in a regular pattern because of the data configuration. In the dimensional approach the conditional variances are larger around the problematic locations (see Figure 17)

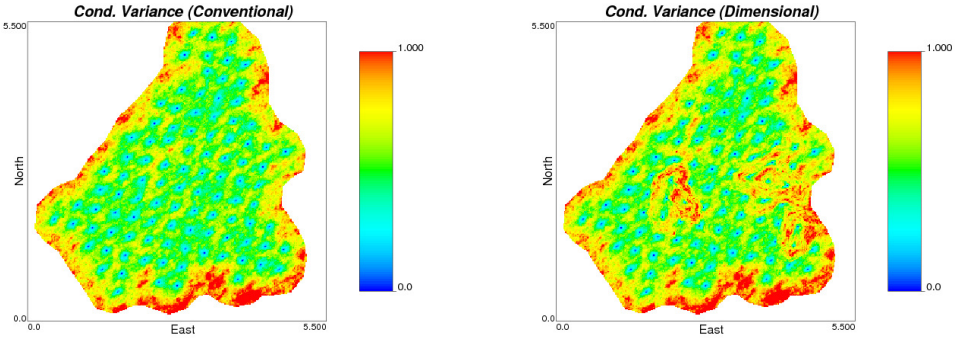

Figure 17: Local conditional variances map of 100 realizations in normal score units of conventional approach (left) and dimensional approach (right)

The proposed approach accounts one second order non-stationary property of the domain, more specifically, the intrinsic hypothesis. Only the regions in the domain where the conditional variability are underestimated are targeted by this approach, which leaves the regions where the variability is over estimated invariant. The reason for this is the extra dimensions where they exist make the data locations more dissimilar than they are in the conventional approach, therefore, increasing the degree of local uncertainty. For reducing the variability there should exist a combination extra dimensions that when they are added makes the separation distances closer than in the original dimensional space, that is not possible using real numbers, however, the use of complex number can be considered which will end up making the problem almost intractable to solve. Moreover, for identifying locations where the local uncertainty is under-estimated it is only necessary to evaluate each data location using cross-validation technique. Whereas, for estimating locations where the local variability is over estimated not one location but many have to be evaluated in order to verify the same condition happens in all of them. From an engineering perspective, the resulting model can be seen as a pessimistic model where the local variability is overestimated.

The non-stationary features are solved by using a stationary methodology. Recall that there is nothing special in the estimation/simulation technique. In the higher dimensional space the domain is assumed and solved as stationary, that is, using a variogram/covariance model and a global symmetric anisotropic pattern. The non-stationary features are highlighted only after the higher dimensional domain is projected onto the original dimensional space. It is worth to mention, the assumption of regionalized variable tries to diminish the impact of additional physical information. Consider in a mineral deposit two data locations are remarkably different because some other geological variable or variables have also suffered also an abrupt change compared to the rest of the domain. In the proposed dimensional approach the extra dimensions try to account that 'reason' of outlier variability in terms of dimensions. That is, two locations are highly variable in the original dimensional space but not as much as variable in the higher dimensional space, the abrupt change in their extra dimensions tries to explain the high variability in the original space. The use of extra dimensions is also another scenario to be modeled as the variable of interest is, there is uncertainty associated to the extra-dimensions. The proposed approach uses a simplistic approach when considers only one scenario of many. However, it is shown that the use of them helps to improve the prediction in terms of performance of the conditional distributions.

Bibliography

Aguilera, A., & Pérez-Aguila, R. (2004). General n-Dimensional Rotations. *WSCG'2004.* Plzen: UNION Agency - Science Press.

Cuba, M., & Leuangthong, O. (2009). *Conditional distribution fitting.* Edmonton: Centre for Computational Geostatistics.

Cuba, M., & Leuangthong, O. (2009). *Experimental variogram cleaning.* Edmonton: Centre for Computational Geostatistics.

Deutsch, C. V., & Journel, A. (1998). *GSLIB Geostatistical Software Library and User's Guide.* New York: Oxford Press.

Goovaerts, P. (1997). *Geostatistics for Natural Resources Evaluation.* New York: Oxford Press.

Isaaks, E., & Srivastava, M. (1989). *An Introduction to Applied Geostatistics.* New York: Oxford Press.